

Elucidation of the Antimicrobial Mechanism of Mutacin 1140

Leif Smith,^{*,‡} Hester Hasper,[§] Eefjan Breukink,[§] Jan Novak,^{||} Jiří Čerkasov,[⊥] J. D. Hillman,[#] Shawanda Wilson-Stanford,[‡] and Ravi S. Oruganty[∇]

Department of Biological Sciences, Mississippi State University, Mississippi State, Mississippi 39762, Department Biochemistry of Membranes, Centre for Biomembranes and Lipid Enzymology, Institute of Biomembranes, Utrecht University, Padualaan 8, 3584 CH Utrecht, The Netherlands, Department of Microbiology, University of Alabama at Birmingham, Birmingham, Alabama 35294, Department of Animal Physiology and Developmental Biology, Charles University, Vinicna 7, 120 00 Prague, Czech Republic, Antimicrobial Division, Oragenics, Inc., Alachua, Florida 32615, and Mass Spectrometry Center, ThermoFisher Scientific, West Palm Beach, Florida 33407

Received June 27, 2007; Revised Manuscript Received December 20, 2007

ABSTRACT: Mutacin 1140 and nisin A are peptide antibiotics that belong to the lantibiotic family. N-Terminal rings A and B of nisin A and mutacin 1140 (lipid II-binding domain) share many structural and sequence similarities. Nisin A binds lipid II and thus disrupts cell wall synthesis and also forms transmembrane pores. Very little is known about mutacin 1140 in this regard. We performed fluorescence-based studies using a bacteria-mimetic membrane system. The results indicated that lipid II monomers are arranged differently in the mutacin 1140 complex than in the nisin A complex. These differences in complex formation may be attributed to the fact that nisin A uses lipid II to form a distinct pore complex, while mutacin 1140 does not form pores in this membrane system. Further experiments demonstrated that the mutacin 1140–lipid II and nisin A–lipid II complexes are very stable and capable of withstanding competition from each other. Transmembrane electrical potential experiments using a *Streptococcus rattus* strain, which is sensitive to mutacin 1140, demonstrated that mutacin 1140 does not form pores in this strain even at a concentration 8 times higher than the minimum inhibitory concentration (MIC). Circular complexes of mutacin 1140 and nisin A were observed by electron microscopy, providing direct evidence for a lateral assembly mechanism for these antibiotics. Mutacin 1140 did exhibit a membrane disruptive function in another commonly used artificial bacterial membrane system, and its disruptive activity was enhanced by increasing amounts of anionic phospholipids.

The increasing occurrence of multidrug-resistant bacteria has created a dramatic need for the identification and testing of new antibiotics to take the place of those that are failing. Mutacin 1140 is a posttranslationally modified peptide antibiotic produced by *Streptococcus mutans* JH1140 (1). It belongs to a family of antibiotics called lantibiotics because of their unique posttranslational modification involving the formation of lanthionine rings. This class of antibiotics has received considerable attention because of their broad spectrum of activity, high potency, low immunogenicity, and good structural stability. Importantly, genetically stable resistant variants of sensitive strains have not yet been found, suggesting that the structure and chemistry of mutacin 1140 may provide important information for the development of new antibiotics. Mutacin 1140 is also a key component in the development of replacement therapy for the prevention of dental caries (2). Thus, for these reasons, it is important to obtain a comprehensive understanding of mutacin 1140 and its mechanism of activity.

The 3-D structure of mutacin 1140 was determined using the membrane-mimetic solvent acetonitrile–water (80:20),

which is a reasonable starting point to predict the orientation of the membrane-bound molecule (3). Similar to nisin A and gallidermin, the thioether ring structures of mutacin 1140 were rigid and well-defined, and the regions not spanned by thioether linkages were quite flexible (4–6). These flexible regions may be important for bactericidal activity by allowing the lantibiotic to orient itself properly in the membrane (7–10) and for complex formation. Mutacin 1140 was determined to have an overall horseshoe-like structure and is approximately 26 Å in length, 14 Å in width, and would be inserted about 17 Å into the membrane.

Electrostatic interactions between the lantibiotic and the bacterial membrane are believed to be important for the initial binding. Experiments with nisin A have demonstrated that the sensitivity of the host bacterium is dependent on the charged state of its cell wall and membrane (7, 10, 11). More importantly, cell–lantibiotic interactions are enhanced by the presence of docking molecules such as lipid II (12–14). Lipid II aids in complex formation and, in the case of nisin A, also in the formation of transmembrane pores. The interaction of nisin A with lipid II involves a novel lipid II binding motif that has been characterized by NMR¹ (15). The N-terminal portion of nisin A, lanthionine rings A and B, interacts with

* To whom correspondence should be addressed. E-mail: jls859@msstate.edu. Fax: (662) 325-7939. Phone: (662) 325-1244.

[‡] Mississippi State University.

[§] Utrecht University.

^{||} University of Alabama at Birmingham.

[⊥] Charles University.

[#] Oragenics, Inc.

[∇] ThermoFisher Scientific.

¹ Abbreviations: MIC, minimum inhibitory concentration; DOPG, 1,2-dioleoyl-*sn*-glycero-3-[phospho-*rac*-(1-glycerol)]; DOPC, 1,2-dioleoyl-*sn*-glycero-3-phosphocholine; NMR, nuclear magnetic resonance; TEM, transmission electron microscopy; LUV(s), large unilamellar vesicle(s); TPP⁺, tetraphenylphosphonium; CF, carboxyfluorescein.

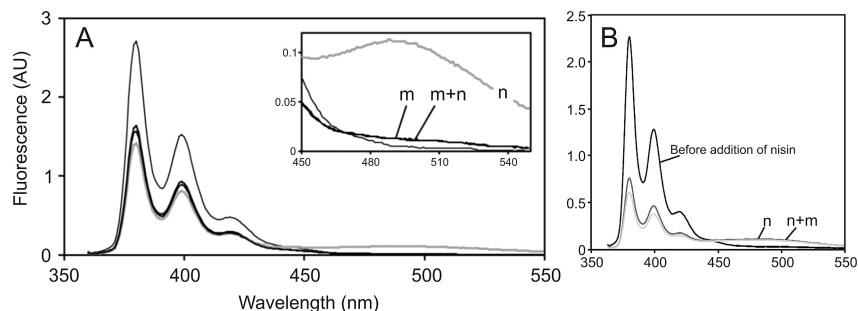


FIGURE 2: Competition assay of excimer fluorescence of pyrene-labeled lipid II. (A) The fluorescence was recorded following incubation for 5 min with $0.75 \mu\text{M}$ mutacin 1140 (tracing m) and compared to pyrene-labeled lipid II fluorescence in the absence of mutacin 1140 or nisin A (thin black tracing). The fluorescence was then recorded after the addition of $0.75 \mu\text{M}$ nisin to the vesicles preincubated with mutacin 1140 (tracing m + n). The gray line (tracing n) represents the fluorescence after addition of $0.75 \mu\text{M}$ nisin A only. The inset shows an enlarged view of the excimer region. There was no increase in the excimer fluorescence of pyrene-labeled lipid II in vesicles incubated with mutacin 1140 and subsequently incubated with nisin A, demonstrating that nisin A cannot abduct lipid II from the mutacin 1140–lipid II complex. (B) Pyrene-labeled lipid II fluorescence was recorded in the absence of nisin A (thin black tracing) and after incubation for 5 min with $0.75 \mu\text{M}$ nisin A (tracing n). The fluorescence was then recorded after the addition of $0.75 \mu\text{M}$ mutacin 1140 to the vesicles preincubated with nisin A (tracing m + n). There was no significant decrease in the excimer fluorescence of pyrene-labeled lipid II following incubation with mutacin 1140, demonstrating that mutacin 1140 cannot abduct lipid II from the nisin A–lipid II complex.

the CF-loaded vesicle suspension to determine maximum fluorescence intensity. Acetonitrile–water (80:20) was used as a negative control. Phospholipid concentration was based on total phosphorus (23).

Mutacin 1140 was dissolved in acetonitrile–water (8:2 and 7:3) at a concentration of 1 mM for the DOPG–DOPC experiments and the LUV experiments, respectively. Nisin A stock solutions were made in 0.05% acetic acid at concentrations of 0.25 and 0.80 mM. All peptide solutions were kept at -20°C until used. Pyrene-labeled lipid II and unlabeled lipid II were synthesized and purified as was previously published (20). Labeled and unlabeled lipid II species were dissolved in chloroform–methanol (1:1 v/v) at concentrations of 0.5–1.0 mM and stored under nitrogen at -20°C . CF and pyrenesulfonyl chloride were obtained from Invitrogen (Carlsbad, CA). Fluorescence measurements for the DOPG–DOPC and LUV experiments were performed with a VersaFluor fluorometer (Bio-Rad, Hercules, CA) and an SLM-Aminco SPF-500 C fluorometer (SLM Instruments Inc., Urbana, IL), respectively. Vesicles were added to 10×4 mm cuvettes in 1.25 mL final volume.

Measurement of the Transmembrane Electrical Potential. The transmembrane electrical potential in cells was determined with an electrode specific for the lipophilic cation tetraphenylphosphonium (TPP^+) (24) as described previously (25). Nigericin, a K^+/H^+ antiporter was used to uncouple the H^+ gradient at a $1 \mu\text{M}$ concentration. Valinomycin, a K^+ -free transporter, served as positive control for dissipation of the K^+ gradient at a $1 \mu\text{M}$ concentration. *S. rattus* BHT-2 (laboratory collection (26)) was used as a mutacin 1140-susceptible strain (27). Cells were grown in trypticase soy broth with yeast extract (Difco Laboratories, Detroit, MI) at 37°C . Cells from early log phase (OD_{600} approximately 0.25) were washed by centrifugation in phosphate-buffered saline (PBS) before the experiment. Mutacin 1140 was added to a final concentration of $8 \mu\text{M}$.

Transmission Electron Microscopy. Negatively stained samples were prepared by floating $20 \mu\text{L}$ of $20 \mu\text{M}$ mutacin 1140 or nisin A solution (acetonitrile–water, 80:20) on a carbon-coated copper grid for 4 min. Excess liquid from each sample was blotted with filter paper, and then the specimens were stained with 2% uranyl acetate for 30 s.

Acetonitrile–water (80:20) was used as a negative control. The mutacin 1140 and nisin A grids were observed under a transmission electron microscope, Jeol JEM-100CXII (Joel Ltd., Tokyo, Japan). Images were taken at magnifications between 40000 and 50000.

RESULTS

Mutacin 1140–Lipid II Complex. The nisin A–lipid II pore complex was previously characterized using pyrene-labeled lipid II. The pyrene-labeled lipid II molecules in these pores were shown to be in close contact, giving rise to an excimer signal with a simultaneous decrease in the monomer signals (20). The activity of mutacin 1140 was further explored using the DOPC LUV model membrane system. To determine whether mutacin 1140 can induce similar excimer signals, as was observed for the nisin A pore complex, we compared the fluorescence of pyrene-labeled lipid II in DOPC LUVs in the presence of mutacin 1140 and nisin A. The fluorescence spectrum of $0.25 \mu\text{M}$ pyrene-labeled lipid II in DOPC vesicles (0.1 mol %) before (thin black line) and 5 min after the addition of a 3-fold excess of mutacin 1140 (line m) exhibited the three characteristic pyrene monomer signals in the 360–440 nm range (see Figure 2A). The decrease in the intensity of the monomer signals following the addition of mutacin 1140 showed that mutacin 1140 was bound to lipid II. However, following the addition of mutacin 1140 the excimer signal between 440 and 550 nm was virtually absent (see Figure 2A, insert, line m) compared to that of nisin A (Figure 2A, insert, line n). The lack of mutacin 1140-induced excimer intensity is most probably due to differences in the way lipid II is oriented during formation of the mutacin 1140–lipid II and nisin A–lipid II complexes. When an equal molar amount of nisin A was added after mutacin 1140, the formation of the intense excimer signal was completely blocked by mutacin 1140 (Figure 2A). This experiment was repeated with vesicles first exposed to nisin A (Figure 2B). However, this time, when an equal molar amount of mutacin 1140 was added after nisin A, there was no disruption of the intense excimer signal by mutacin 1140 (Figure 2B). These data showed that mutacin 1140 and nisin A complexes tightly sequestered lipid II and could not be competitively replaced.

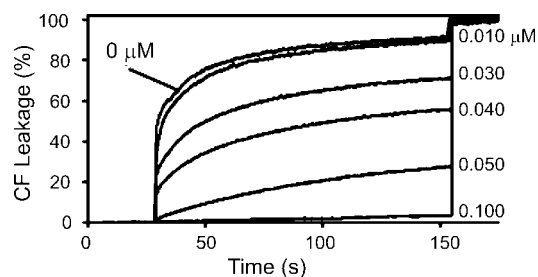


FIGURE 3: Mutacin 1140 and nisin A competition assay for lipid II. Leakage induced by nisin A was inhibited by equal molar concentrations of mutacin 1140. The LUVs containing DOPC and 0.1 μM lipid II were incubated for 5 min with various mutacin 1140 concentrations (0.010–0.100 μM), while nisin A was subsequently added at a 0.100 μM concentration. Fluorescence of samples containing CF-loaded DOPC vesicles was recorded for 200 s. From a 20% Triton X-100 solution, 10 μL was added to yield the value for 100% leakage.

In previous studies, CF release experiments using LUVs composed of the synthetic lipid DOPC with 0.1 mol % lipid II revealed that micromolar concentrations of mutacin 1140 were not able to form a pore (16). The lack of any noticeable pore formation by mutacin 1140 contrasts the effects seen with nisin A, as this lantibiotic causes an efficient release of CF at nanomolar concentrations (14). Because mutacin 1140 was not capable of producing a pore large enough for the efflux of CF from LUVs (16), we were able to design a competition assay in which we measured the ability of mutacin 1140 to inhibit nisin A from forming a transmembrane pore. This was done by monitoring the nisin A-induced efflux of CF with vesicles incubated with varying concentrations of mutacin 1140 (Figure 3). These experiments revealed that the addition of 0.1 μM nisin A to vesicles incubated with mutacin 1140 resulted in leakage only when the mutacin 1140 concentration dropped below the lipid II concentration (0.1 μM). This corresponds to a 1:1 stoichiometry if all lipid II molecules were available for the interaction with mutacin 1140. This 1:1 stoichiometry has also been previously described for nisin A and lipid II (21, 28). Similar to what was revealed in the pyrene-labeled lipid II experiments, the stability of the mutacin 1140–lipid II complexes is high enough to withstand the competition by nisin A in these CF release experiments.

Mutacin 1140 Membrane Studies. To characterize mutacin 1140's action in the membrane, we used potentiometric measurements with a K^+ electrode and TPP^+ electrode. As previously reported, mutacin 1140 at concentrations ranging from 0.1 to 1.0 μM was unable to induce CF leakage in the *in vitro* DOPC LUV membrane system containing 0.1 mol % lipid II (16). Given the possibility that the pores could be too small to allow for the efflux of CF, K^+ leakage experiments were done utilizing the same *in vitro* model membrane system. In these experiments, mutacin 1140 was also unable to induce K^+ leakage (data not shown). Mutacin 1140 was tested at the upper limit concentration of 1.0 μM , which is 10-fold higher than the concentration reported for pore formation induced by nisin A. To study whether mutacin 1140 is capable of permeabilizing the cytoplasmic membrane, we used the susceptible strain *S. rattus*. This strain has been used for over 2 decades as an indicator strain for mutacin 1140 activity (1, 27). The MIC for mutacin 1140 against *S. rattus* in early log phase (OD_{600} approximately 0.25) is <1 $\mu\text{g}/\text{mL}$. Mutacin 1140's effect on the transmembrane electri-

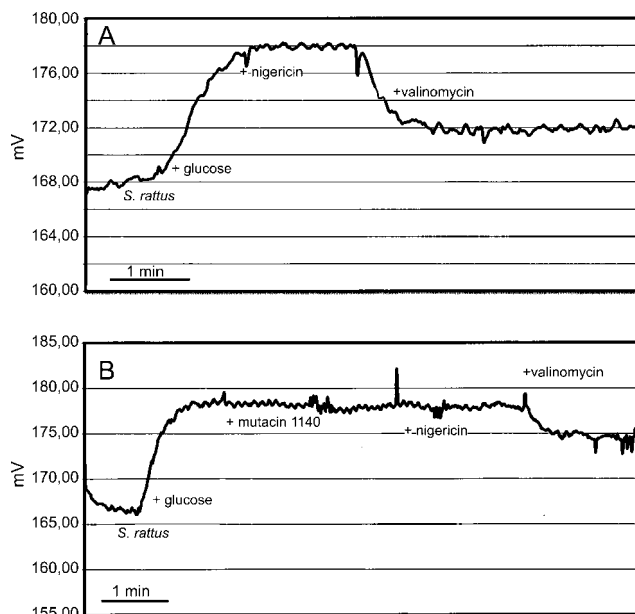


FIGURE 4: Measurement of transmembrane potential using a TPP^+ electrode. (A) Control experiment with *S. rattus* cells. Glucose was added to energize the cells, nigericin, a K^+/H^+ antiporter, was used to uncouple the H^+ gradient, and valinomycin, a K^+ free transporter, served as positive control for dissipation of the K^+ gradient. (B) Mutacin 1140 added to the glucose-energized cells caused a negligible change in the transmembrane potential, showing that mutacin 1140 did not permeabilize the membrane of the sensitive strain.

cal potential was determined by monitoring the distribution of the lipophilic cation TPP^+ in energized *S. rattus* cells during early log phase. First, a control experiment was performed with glucose-energized cells incubated with nigericin followed by the addition of valinomycin, uncoupling the transmembrane electrical potential (Figure 4A). Using a high concentration of mutacin 1140 (8 μM), we showed that the transmembrane electrical potential of susceptible glucose-energized *S. rattus* cells was not depolarized by the addition of mutacin 1140 (Figure 4B). The potassium ionophore valinomycin elicited an instantaneous dissipation of the transmembrane electrical potential, indicating that the experimental system was fully functional. This experiment demonstrated that mutacin 1140 does not form a pore complex in the sensitive strain *S. rattus*. These results support an alternative bactericidal mechanism other than pore formation for mutacin 1140, likely involving lipid II abduction.

To further examine the possibility of mutacin 1140's ability to disrupt membranes, we used the bacteria-mimetic DOPG–DOPC membrane system that was first utilized for characterization of nisin A's pore-forming ability (8). This membrane system demonstrated that mutacin 1140 can permeabilize membranes, depending on anionic lipid content. The percentage of CF release from 100% DOPG vesicles with a 3 μM lipid concentration was determined 5 min after the addition of varying concentrations of mutacin 1140 (Figure 5A). Efficient release of CF was observed at low concentrations of mutacin 1140; $\sim 46\%$ of the CF was released in 5 min from vesicles exposed to mutacin 1140 at a 435 nM concentration. At this concentration, release of CF was observed when there was at least one mutacin 1140 molecule per seven DOPG molecules. The vesicles were depleted of CF at a 1.4 μM concentration of mutacin 1140

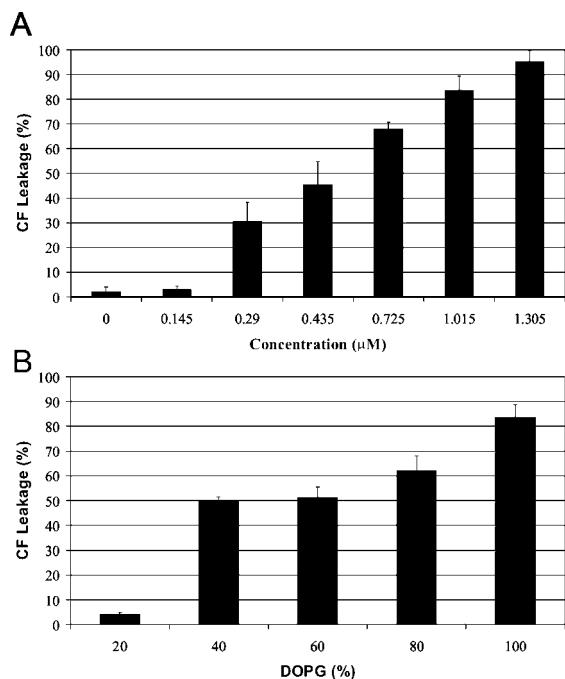


FIGURE 5: Bacteria-mimetic DOPG–DOPC membrane studies. (A) Induced leakage of CF from 100% DOPG vesicles with increasing concentrations of mutacin 1140. (B) Induced leakage of CF from vesicles with varying ratios of DOPG–DOPC with a constant concentration of mutacin 1140 (1 μM). CF release was determined 5 min after the addition of mutacin 1140. Each data point is the average of three separate experiments. Lipid concentration was 3 μM (expressed as total P_i).

in 5 min. Interestingly, no significant CF release was detected until reaching a 145 nM mutacin 1140 concentration. This suggested that there was a threshold concentration (more than 1 mutacin 1140 molecule per 20 DOPG molecules) for complex formation that disrupted the DOPG vesicle membrane. We also examined the dependency of mutacin 1140 activity on anionic phospholipid by varying the percentage of the anionic phospholipid DOPG relative to the zwitterionic phospholipid DOPC (Figure 5B). CF release increased with increased proportion of DOPG at a constant lipid to mutacin 1140 ratio. The maximum efficiency of CF release was observed with 100% DOPG vesicles. There was a small release of CF from the 20% DOPG vesicles. The dramatic decrease in activity observed with the 20% DOPG vesicles suggested that anionic phospholipids were important for the membrane-disrupting activity of mutacin 1140 in the DOPG–DOPC membrane system and that anionic phospholipids enhanced the membrane perturbation effects.

Complex Formation Observed by Electron Microscopy.

TEM was initially performed to visualize pore complexes on vesicle membranes. Although no pore complexes were observed with TEM, mutacin 1140's ability to disrupt DOPG–DOPC vesicles was detected (data not shown). Further examination of these grids showed unusual circular objects in the background. In an attempt to identify the source of these objects, a carbon-coated grid was floated on a sample of mutacin 1140 in acetonitrile–water (80:20) for 4 min and stained. Interestingly, large circular objects averaging 50 nm in diameter were present on these grids (Figure 6A) but absent from the acetonitrile–water (80:20) negative control. The covalent and three-dimensional structures of mutacin 1140 were determined by nuclear magnetic resonance using

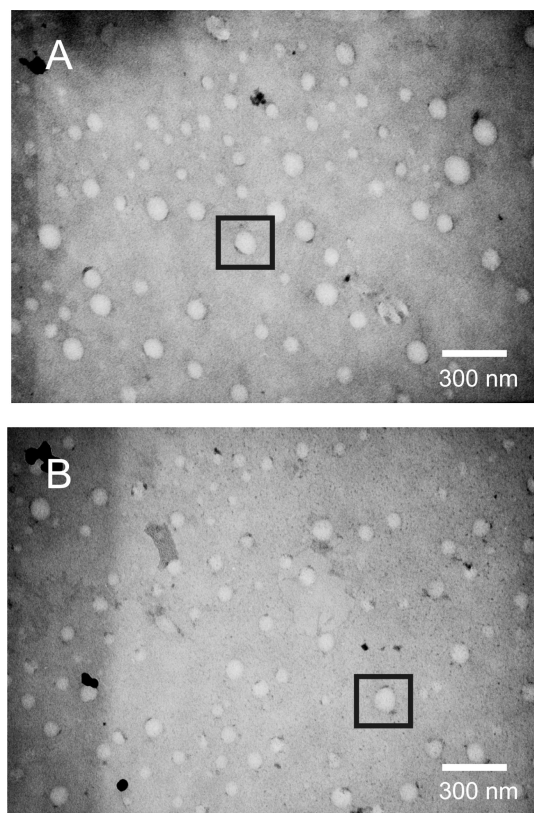


FIGURE 6: TEM micrographs of mutacin 1140 and nisin A complexes. (A) The carbon-coated grid was floated on 20 μL of a 20 μM mutacin 1140 solution (acetonitrile–water, 80:20) for 4 min and was stained with 2% uranyl acetate for 30 s. (B) The carbon-coated grid was floated on 20 μL of a 20 μM nisin A solution (acetonitrile–water, 80:20) for 4 min and was stained with 2% uranyl acetate for 30 s. Mutacin 1140 and nisin A formed circular complexes on the grids. A black box is drawn around each of these complexes.

the same solvent conditions (3, 29). These data provide evidence that mutacin 1140 exists as a monomer in solution since all samples had narrow line widths and did not show any changes in chemical shift when mutacin 1140 was diluted (3). A mechanism for lateral assembly is the only plausible explanation for the large circular geometry seen by TEM. This assembly may be activated by exposure to the hydrophobic carbon-coated grid. At best, a very rough guess can be made at estimating the relative number of mutacin 1140 monomers in these complexes. The dimensions of mutacin 1140 were previously determined from the three-dimensional NMR structural analysis and were estimated to be 26 \times 14 \AA in width and 17 \AA in depth (3). On the basis of the maximum area that the widths of each monomer would occupy, each complex may contain more than 100 monomers of mutacin 1140. We repeated these experiments with nisin A and found that it also formed similar large uniform complexes on the grid (Figure 6B). The nisin A complexes were also approximately 50 nm in diameter and, thus, also contain a high number of nisin A monomers. These structures on the carbon-coated grid show that mutacin 1140 and nisin A have an inherent ability for lateral assembly. This attribute further explains why nisin A or mutacin 1140 could not abduct lipid II after the vesicles were pre-exposed to them in the competition assays described above. Presumably, the lateral interactions of mutacin 1140 and nisin A promote

formation of an extremely tight complex that locks in lipid II, preventing competition for lipid II from nisin A or mutacin 1140.

DISCUSSION

The findings from this study include experiments showing the following: a distinct difference in the positioning of lipid II in the mutacin 1140 complex and the nisin A complex; competition studies that demonstrate the stability of mutacin 1140–lipid II and nisin A–lipid II complexes; a membrane potential study on a mutacin 1140-sensitive strain demonstrating that mutacin 1140 kills this strain by a mechanism other than pore formation; mutacin 1140's ability to disrupt the DOPG–DOPC membranes, which improves with increasing anionic lipid content; and mutacin 1140 and nisin A's inherent ability to form large circular complexes as observed by TEM. These data suggest that mutacin 1140 kills bacteria primarily by lipid II abduction and may also kill by a membrane-disruptive mechanism; albeit the latter mechanism has not been observed *in vivo*.

Using the DOPC LUV experimental system, we showed that pyrene-labeled lipid II lacked an excimer signal following the addition of mutacin 1140 and that the mutacin 1140– and nisin A–lipid II complexes were very stable. The lack of a lipid II excimer signal following addition of mutacin 1140 was different from nisin A, suggesting either that lipid II monomers must be located farther apart in the mutacin 1140 complexes than in the nisin A complexes, even though mutacin 1140 (22 amino acid residues) is considerably smaller than nisin A (34 amino acid residues), or that the orientation of the lipid II headgroup is different. One important distinction between nisin A and mutacin 1140 is that nisin A monomers, in the presence of lipid II, can span the bilayer forming an actual pore complex, while experimental evidence suggests that there is no pore complex for mutacin 1140 in the DOPC LUV system. Therefore, the pyrene excimer signal is most probably a characteristic of the formation of an actual pore complex.

The N-terminal portion of mutacin 1140 and nisin A, comprising rings A and B, represents the lipid II binding motif (Figure 1). The sequence variability outside of the lipid II binding domain likely confers the functionality of the lantibiotic, in particular, whether it is a pore former, and how it positions lipid II during complex formation. In addition to a lipid II binding domain, our work supports the belief that there is a separate binding motif for lateral association of these lantibiotics. This dual activity of binding to lipid II followed by lateral assembly of the lantibiotic may explain the high potency of these antimicrobial compounds. The binding affinity for nisin A to lipid II has been calculated to be in the order of $2 \times 10^7 \text{ M}^{-1}$ (14). This binding affinity does not take into consideration the lateral assembly of the lantibiotic which would further trap lipid II into large lantibiotic islands in the bilayer. This bactericidal mechanism of activity ensures that lipid II will not become available for cell wall synthesis.

We did not see an effect on membrane potential when mutacin 1140 was added to a mutacin 1140-susceptible strain *S. rattus*. This differs significantly from nisin, which elicits a dramatic drop in membrane potential in *Staphylococcus cohnii* (31). The difference in activity is that nisin A actually

forms a stable pore complex (20). Although similar to nisin A (8), mutacin 1140 did demonstrate a potent membrane-disruptive capability in the DOPG–DOPC membrane system that was dependent on anionic lipid content. Mutacin 1140's ability to disrupt the DOPG–DOPC model membranes suggests that it may kill by a membrane-disruptive mechanism, although we should emphasize that the DOPG–DOPC model membrane system has a much lower membrane stability than a bacterial membrane. The electrostatic attraction of mutacin 1140 to the negatively charged headgroups presumably increases the rate in which mutacin 1140 binds to the membranes, thus promoting membrane disruption. Supporting data come from the binding affinities of nisin A to this model membrane system. The interaction of radio-labeled nisin Z to 100% DOPC vesicles was 10-fold less than for 100% DOPG vesicles (8).

The relative importance of anionic lipid content for the antimicrobial activity of mutacin 1140 and other lantibiotics is not well understood. For instance, the bacterium *Listeria monocytogenes* was shown to be relatively insensitive to nisin A (MIC between 200 and 1000 $\mu\text{g/L}$) even though the content of the negatively charged lipids is relatively high, i.e., reported to be 50–88% (8, 32). Therefore, other factors besides anionic lipid content may affect the sensitivity of a bacterium to lantibiotics. The thickness and composition of the cell wall and cell membrane could be another important determinant for bacterial susceptibility (8, 17). The role of negatively charged lipids in the antimicrobial activity of mutacin 1140, as well as other lantibiotics, would require further examination. The importance of membrane composition, in particular anionic membrane composition, for the antimicrobial peptide protegrin-1 was described recently (33).

Interestingly, mutacin 1140 and nisin A were shown to form uniform circular complexes, composed of more than 100 monomers on the TEM grid. These complexes form after the lantibiotic makes contact with the hydrophobic carbon film on the grids and provide direct visualization of the lateral assembly of mutacin 1140 and nisin A. Direct visualization by TEM can be used in future mutagenesis studies to identify the residues important for the assembly process. An inherent mechanism for lateral assembly of these antibiotics helps to explain the abduction and clustering of lipid II in bacteria and bacteria-mimetic membrane systems (16). It also helps to explain the stability of mutacin 1140–lipid II and nisin A–lipid II complexes and why they are very effective bactericidal compounds. Not only do they have a dedicated lipid II binding domain, but they also assemble into large complexes that trap lipid II into a lantibiotic cage, thus, permanently removing lipid II from the site of bacterial cell wall synthesis. Type B lantibiotics, in particular, actagardine and mersacidin, have also been shown to function without forming pores and are believed to bind to lipid II, thus inhibiting cell wall inhibition (30).

In conclusion, mutacin 1140's primary mode of bactericidal activity is presumably through the binding of lipid II and trapping it into a tight lantibiotic cage complex, which, in turn, blocks cell wall synthesis. This hypothesis is based on the observation that mutacin 1140 did not affect the membrane potential of the mutacin 1140-sensitive strain *S. rattus* and that mutacin 1140 sequesters lipid II into a stable complex. Furthermore, we showed that mutacin 1140 and nisin A both have an inherent ability to form large circular

complexes on a carbon-coated grid, suggesting that they have a distinct mechanism for lateral assembly. These experiments expand our knowledge of the function of mutacin 1140. In addition, it promotes future areas of study for mutacin 1140, as well as other lantibiotics, that will enhance our understanding of the mechanisms involved in the lateral assembly process, which plays an important role in trapping lipid II.

ACKNOWLEDGMENT

The authors thank Dr. Arnold Driessen, University of Groningen, Haren, The Netherlands, for advice on the construction of a TPP⁺ electrode and a gift of the TPP⁺-specific membrane. The authors also appreciate the expert help from Ing. Jiri Hucl with software for recording the electrode measurements. The authors thank Dr. Arthur Edison, University of Florida, for learned advice. The authors also thank the staff of the Electron Microscopy Facilities at the University of Florida and Mississippi State University.

REFERENCES

- Hillman, J. D., Novak, J., Sagura, E., Gutierrez, J. A., Brooks, T. A., Crowley, P. J., Hess, M., Azizi, A., Leung, K. P., Cvitkovitch, D., and Bleiweis, A. S. (1998) Genetic and biochemical analysis of mutacin 1140, a lantibiotic from *Streptococcus mutans*. *Infect. Immun.* 66, 2743–2749.
- Hillman, J. D., Brooks, T. A., Michalek, S. M., Harmon, C. C., Snoep, J. L., and van der Weijden, C. C. (2000) Construction and characterization of an effector strain of *Streptococcus mutans* for replacement therapy of dental caries. *Infect. Immun.* 68, 543–549.
- Smith, L., Zachariah, C., Thirumoorthy, R., Rocca, J., Novak, J., Hillman, J. D., and Edison, A. S. (2003) Structure and dynamics of the lantibiotic mutacin 1140. *Biochemistry* 42, 10372–10384.
- Freund, S., Jung, G., Gutbrod, O., Folkers, G., Gibbons, W. A., Allgaier, H., and Werner, R. (1991) The solution structure of the lantibiotic gallidermin. *Biopolymers* 31, 803–811.
- van den Hooven, H. W., Spronk, C., van de Kamp, M., Konings, R. N. H., Hilbers, C. W., and van de Ven, F. J. M. (1996) Surface location and orientation of the lantibiotic nisin bound to membrane-mimicking micelles of dodecylphosphocholine and of sodium dodecylsulphate. *Eur. J. Biochem.* 235, 394–403.
- van de Ven, F. J. M., van den Hooven, H. W., Konings, R. N. H., and Hilbers, C. W. (1991) NMR studies of lantibiotics. The structure of nisin in aqueous solution. *Eur. J. Biochem.* 202, 1181–1188.
- Breukink, E., van Kraaij, C., van Dalen, A., Demel, R. A., Siezen, R. J., de Kruijff, B., and Kuipers, O. P. (1998) The orientation of nisin in membranes. *Biochemistry* 37, 8153–8162.
- Breukink, E., van Kraaij, C., Demel, R. A., Siezen, R. J., Kuipers, O. P., and de Kruijff, B. (1997) The C-terminal region of nisin is responsible for the initial interaction of nisin with the target membrane. *Biochemistry* 36, 6968–6976.
- Moll, G. N., Roberts, G. C. K., Konings, W. N., and Driessen, A. J. M. (1996) Mechanism of lantibiotic-induced pore-formation. *Antonie Van Leeuwenhoek* 69, 185–191.
- Montville, T. J., and Chen, Y. (1998) Mechanistic action of pediocin and nisin: recent progress and unresolved questions. *Appl. Microbiol. Biotechnol.* 50, 511–519.
- Abee, T. (1995) Pore-forming bacteriocins of Gram-positive bacteria and self-protection mechanisms of producer organisms. *FEMS Microbiol. Lett.* 129, 1–9.
- Breukink, E., Bonev, B. B., Wiedemann, I., Sahl, H. G., Watts, A., and de Kruijff, B. (2001) Specific interaction of the lantibiotic nisin with lipid II leads to highly efficient pore formation. *Biophys. J.* 80, 7.
- Breukink, E., and de Kruijff, B. (2006) Lipid II as a target for antibiotics. *Nat. Rev. Drug Discov.* 5, 321–332.
- Breukink, E., Wiedemann, I., van Kraaij, C., Kuipers, O. P., Sahl, H. G., and de Kruijff, B. (1999) Use of the cell wall precursor lipid II by a pore-forming peptide antibiotic. *Science* 286, 2361–2364.
- Hsu, S. T. D., Breukink, E., Tischenko, E., Lutters, M. A. G., de Kruijff, B., Kaptein, R., Bonvin, A., and van Nuland, N. A. J. (2004) The nisin-lipid II complex reveals a pyrophosphate cage that provides a blueprint for novel antibiotics. *Nat. Struct. Mol. Biol.* 11, 963–967.
- Hasper, H. E., Kramer, N. E., Smith, J. L., Hillman, J. D., Zachariah, C., Kuipers, O. P., de Kruijff, B., and Breukink, E. (2006) An alternative bactericidal mechanism of action for lantibiotic peptides that target lipid II. *Science* 313, 1636–1637.
- Bonelli, R. R., Schneider, T., Sahl, H. G., and Wiedemann, I. (2006) Insights into in vivo activities of lantibiotics from gallidermin and epidermin mode-of-action studies. *Antimicrob. Agents Chemother.* 50, 1449–1457.
- Kuipers, O. P., Rollema, H. S., Yap, W. M. G. J., Boot, H. J., Siezen, R. J., and de Vos, W. M. (1992) Engineering dehydrated amino acid residues in the antimicrobial peptide nisin. *J. Biol. Chem.* 267, 24340–24346.
- Mulders, J. W. M., Boerrigter, I. J., Rollema, H. S., Siezen, R. J., and de Vos, W. M. (1991) Identification and characterization of the lantibiotic nisin Z, a natural nisin variant. *Eur. J. Biochem.* 201, 581–584.
- Breukink, E., van Heusden, H. E., Vollmerhaus, P. J., Swiezewska, E., Brunner, L., Walker, S., Heck, A. J. R., and de Kruijff, B. (2003) Lipid II is an intrinsic component of the pore induced by nisin in bacterial membranes. *J. Biol. Chem.* 278, 19898–19903.
- Hasper, H. E., de Kruijff, B., and Breukink, E. (2004) Assembly and stability of nisin-Lipid II pores. *Biochemistry* 43, 11567–11575.
- Driessen, A. J. M., van den Hooven, H. W., Kuiper, W., van de Kamp, M., Sahl, H. G., Konings, R. N. H., and Konings, W. N. (1995) Mechanistic studies of lantibiotic-induced permeabilization of phospholipid-vesicles. *Biochemistry* 34, 1606–1614.
- Chen, P. S., Toribara, T. Y., and Warner, H. (1956) Microdetermination of phosphorus. *Anal. Chem.* 28, 1756–1758.
- Shinbo, T., Kamo, N., Kurihara, K., and Kobatake, Y. (1978) A PVC-based electrode sensitive to DDA⁺ as a device for monitoring the membrane potential in biological systems. *Arch. Biochem. Biophys.* 187, 414–422.
- Chikindas, M. L., Garcia-Garcera, M. J., Driessen, A. J. M., Ledebroer, A. M., Nissen-Meyer, J., Nes, I. F., Abee, T., Konings, W. N., and Venema, G. (1993) Pediocin PA-1, a bacteriocin from *Pediococcus acidilactici* PAC1.O, forms hydrophilic pores in the cytoplasmic membrane of target cells. *Appl. Environ. Microbiol.* 59, 3577–3584.
- Hillman, J. D. (1978) Lactate dehydrogenase mutants of *Streptococcus mutans*: isolation and preliminary characterization. *Infect. Immun.* 21, 206–212.
- Hillman, J. D., Johnson, K. P., and Yaphe, B. I. (1984) Isolation of a *Streptococcus mutans* strain producing a novel bacteriocin. *Infect. Immun.* 44, 141–144.
- Hsu, S. T., Breukink, E., de Kruijff, B., Kaptein, R., Bonvin, A., and van Nuland, N. A. J. (2002) Mapping the targeted membrane pore formation mechanism by solution NMR: The nisin Z and lipid II interaction in SDS micelles. *Biochemistry* 41, 7670–7676.
- Smith, L., Novak, J., Rocca, J., McClung, S., Hillman, J. D., and Edison, A. S. (2000) Covalent structure of mutacin 1140 and a novel method for the rapid identification of lantibiotics. *Eur. J. Biochem.* 267, 6810–6816.
- McAuliffe, O., Ross, R. P., and Hill, C. (2001) Lantibiotics: structure, biosynthesis and mode of action. *FEMS Microbiol. Lett.* 25, 285–308.
- Ruhr, E., and Sahl, H. G. (1985) Mode of action of the peptide antibiotic nisin and influence on the membrane-potential of whole cells and on cytoplasmic and artificial membrane-vesicles. *Antimicrob. Agents Chemother.* 27, 841–845.
- Winkowski, K., Ludescher, R. D., and Montville, T. J. (1996) Physicochemical characterization of the nisin-membrane interaction with liposomes derived from *Listeria monocytogenes*. *Appl. Environ. Microbiol.* 62, 323–327.
- Mani, R., Cady, S. D., Tang, M., Waring, A. J., Lehrert, R. I., and Hong, M. (2006) Membrane-dependent oligomeric structure and pore formation of β -hairpin antimicrobial peptide in lipid bilayers from solid-state NMR. *Proc. Natl. Acad. Sci. U.S.A.* 103, 16242–16247.